

PACS numbers: 52.50.Jm; 52.38.Mf; 42.62.Cf
DOI: 10.1070/QE2001v031n05ABEH001958

The role of plasma in ablation of materials by ultrashort laser pulses

S M Klimentov, T V Kononenko, P A Pivovarov, S V Garnov,
V I Konov, A M Prokhorov, D Breitling, F Dausinger

***Abstract*. The ablative formation of deep channels in steel by femtosecond and picosecond laser pulses is studied. A significant screening of the incident energy inside deep channels is found to occur due to the air breakdown at ablated microparticles. The breakdown thresholds and the microparticle precipitation times are estimated. This kind of plasma screening stabilises the linear ablation rate and causes a significant channel broadening.**

Keywords: *ablation, femtosecond laser pulses, laser plasma.*

1. Introduction

The potential advantages of femtosecond laser pulses for material ablation are the subject of wide discussion in the literature [1 – 6]. These advantages are based on the assumption about the absence of plasma-induced screening of laser radiation and an extremely small depth of material heating during the laser irradiation. The consequences are a small depth of the melt or its complete absence, the possibility to transfer the radiation energy directly to the thin layer of the evaporated material, and eventually a high precision of processing limited only by diffraction effects.

Upon irradiation of metals by $\sim$ 100-fs laser pulses, the depth of thermal action may indeed become comparable to the radiation penetration depth l_0 in the material. In many practical cases, $l_0 \leqslant 10^{-5} - 10^{-6}$ cm. The distance l_T of thermal action estimated in the first approximation from the heat conduction relationship $\left[l_T \approx (\chi\tau)^{1/2}\right]$ appears to be smaller: for the thermal diffusivity $\chi \simeq$ cm^2, this distance is $l_T \sim 3 \times 10^{-7}$ cm.

However, the advantages of precision ablation by ultrashort pulses can be realised only for a low irradiation intensity. When the energy density considerably exceeds the threshold value (~ 0.05 J cm^{-2} for steel at $\tau \sim 100$ fs), an intense plasma formation occurs and a combination of processes involved in the femtosecond laser ablation is substantially complicated. In particular, as noted in Ref. [7], it is the plasma action after the termination of a femtosecond laser pulse that can result in the production of significant melt layers, thereby lowering the quality of metal processing.

An important aspect of the problem is that many practical tasks of material microprocessing require high ablation rates and energy densities (10 – 1000 J cm^{-2}). Because the structures to be produced quite often are narrow and deep channels, the resulted laser plasma interacts not only with the irradiated surface, but with the side walls as well.

As shown below, the picture of ablative plasma production by ultrashort laser pulses is complicated still further due to afterpulse effects, which are caused by the accumulation of microparticles or ablated clusters in the atmosphere and are hardly avoidable in the production of deep channels in the air. As a consequence, the irradiation by subsequent radiation pulses may lead to a low-threshold optical breakdown of the air containing microparticles and to a simultaneous appearance of two plasma clouds. One of them is a conventional near-surface plasma plume at the bottom of the channel and the other is a plasma cloud, which is located at a considerable distance from the former inside the channel near its axis.

The role of plasma screening in the ablation by intense picosecond laser pulses was earlier investigated in Ref. [8]. The aim of this work is to study experimentally and compare the above-mentioned properties of plasma production upon the material ablation by femtosecond and picosecond laser pulses.

2. Experimental

We used in our experiments a 'Spectra Physics' Hurricane femtosecond laser emitting 800-nm, 130-fs pulses and a Nd:YAG laser emitting 300-ps pulses. The pulse repetition rate was 1 kHz for the femtosecond laser and 5 Hz for the picosecond laser. In accordance with the layout of the measurements shown schematically in Fig. 1, the laser radiation with a nearly Gaussian profile was focused on the surface of a carbon-steel sample (*1*) placed on the input window (*2*) of an integrating sphere (*3*). The radiation was focused with lenses (*4*) with focal lengths 50 – 110 mm, the beam waist diameter d_w being equal to 18 – 40 μm at the $1/e^2$ intensity level. Upon the production of a through channel, the radiation entering the sphere (*3*) was transmitted to photodiode (*6*) via optical fibre (*5*). A photodiode (*7*) was used to measure the incident energy. The recording system outlined above allowed us to determine the linear ablation rate, to measure the optical transmission of the resultant through channels, and to study the screening properties of

S M Klimentov, T V Kononenko, P A Pivovarov, S V Garnov, V I Konov, A M Prokhorov Institute of General Physics, Russian Academy of Sciences, ul. Vavilova 38, 119991 Moscow, Russia; fax: (095) 135 76 72
D Breitling, F Dausinger Institut fur Strahlwerkzeuge, Pfaffenwaldring 43, D-70569 Stuttgart, Germany; fax: +49 (0711) 685 68 42

Received 14 March 2001
Kvantovaya Elektronika **31** (5) 378 – 382 (2001)
Translated by E N Ragozin

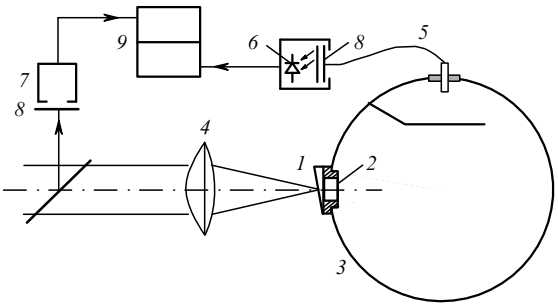

Figure 1. Schematic for measuring the optical transmission of ablated channels: (*1*) wedged sample; (*2*) input window; (*3*) integrating sphere; (*4*) focusing lens; (*5*) optical fibre; (*6*) *pin* photodiode; (*7*) energy meter; (*8*) optical filters; (*9*) analogue-to-digital converter.

the plasma inside them. Earlier this measurement technique was successfully used to study the ablation of transparent and nontransparent materials (steel, ceramics, polycrystalline diamond films) irradiated by nanosecond and picosecond laser pulses, as well as by a combination of laser pulses of different duration [9, 10].

As an example, Fig. 2 shows the typical dependences of the sample transmission on the number of picosecond laser pulses. The formation of a through channel is indicated by the increase of the radiation energy that enters the sphere. The number of pulses corresponding to this instant of time permits obtaining the average linear ablation rate for a sample of a given thickness. The continuing signal growth indicates that the output opening broadens, while the attainment of a stationary magnitude means the completion of this process. One of the dependences shown in Fig. 2 was obtained for a low radiation intensity, which did not exceed the material ablation threshold, and characterises the so-called cold transmission T_c of the channels produced. The other dependence was obtained for an ablation-driving intensity and characterises, apart from the component related to the losses in the channels, the screening of the incident radiation by the plasma being produced. This will be referred to as a 'hot' transmission and conventionally designated T_h. It follows from Fig. 2 that after completion of the formation of the output opening, whose diameter is many times greater than d_w, the 'hot' and 'cold' transmission do not coincide and $\sim 90\,\%$ of the incident energy is scattered and absorbed by the plasma inside the channel.

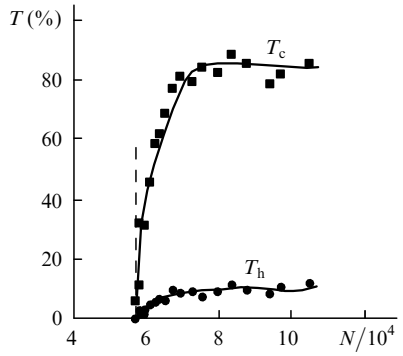

Figure 2. Dependences of the optical transmission of a channel on the number of picosecond ablation pulses for a radiation intensity above (T_h) and below (T_c) the ablation threshold.

3. Experimental results

Fig. 3 shows the dependences of the average ablation rate on the energy density obtained using the above technique for $\tau = 130$ fs in steel. Irrespective of the sample thickness δ, there are two characteristic portions in the curves: the first portion, in which the rate increases sharply as the energy density J increases up to $25-30$ J cm^{-2}, and the next comparatively flat portion, in which the ablation rate no longer depends on the incident energy. Such a sharp transition can be explained by comparing the dependences of the 'hot' and 'cold' transmission presented in Fig. 4 for the through ablation channels in a plate with a thickness $\delta = 200$ μm. Recall that all the experimental measurements here correspond to the total aperture of the ouput opening.

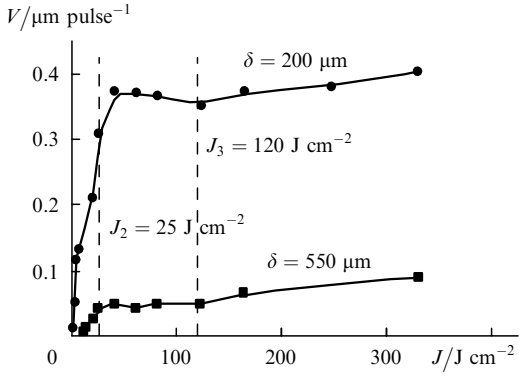

Figure 3. Dependences of the average linear ablation rate on the laser energy density in the case of 130-fs pulses for samples with thickness $\delta = 200$ and 550 μm.

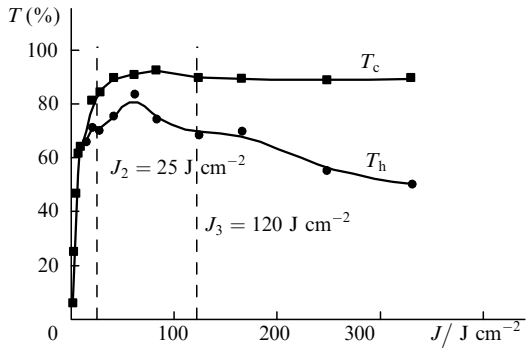

Figure 4. Dependences of the 'cold' (T_c) and 'hot' (T_h) transmission of through channels in a sample with a thickness $\delta = 200$ μm on the incident energy density for $\tau = 130$ fs.

One can see that the transmissions coincide ($T_c = T_h$) up to $J = 20 - 25$ J cm^{-2}, which suggests that there is no appreciable screening of the ablation-driving radiation. As the energy density increases, the 'cold' transmission continues to increase and approaches 100 %, because the diameter of the channels being produced also increases and already exceeds the diameter of the laser beam waist $d_w = 18$ μm by a factor of $4-6$. This fact is illustrated by the images of input and output openings in Fig. 5. Despite the formation of relatively broad channels, T_h in this case becomes lower than T_c and decreases further with increasing energy density. Note that the observed screening cannot be attributed to the

ablation of the side walls. First, off-the-wall plasma has no time to reach the channel axis during irradiation by a femtosecond laser pulse. Second, even in the case of 'hot' measurements, the energy density at the walls (in the wings of the Gaussian distribution) is below the threshold level $J_1 = 0.05$ J cm^{-2}.

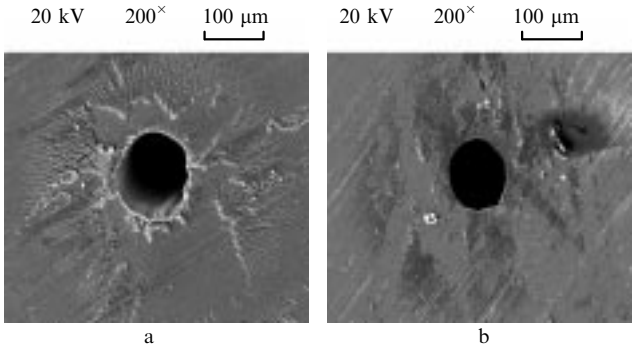

Figure 5. Entrance (a) and exit (b) openings in a 200-μm thick steel sample for $\tau = 130$ fs and $J = 170$ J cm^{-2}.

Therefore, the curves T_h and T_c differ from each other because of the air breakdown inside the channel. The low breakdown threshold or, to be more precise, the screening threshold ($J_2 = 20 - 25$ J cm^{-2}) can be explained by the presence of ablation particles inside the channel, which are capable of initiating the development of an electron avalanche in a gas, as noted for long laser pulses (see, for instance, Ref. [11]). Fig. 6 shows for comparison the dependence of the transmission of pure air that did not contain microparticles (without a sample on the input window of the sphere) on the incident energy density. In this case, a significant screening ($\Delta T \sim 10$ %) owing to the air breakdown sets in only for $J_3 = 120$ J cm^{-2}. A comparison of Figs 3–6 shows that the characteristic features manifest themselves in all plots for the energy densities J_2 and J_3. The laser-induced air breakdown at the particles inside the channel corresponds to a cessation in the growth of the ablation rate, while the breakdown of the pure air above the surface of a sample corresponds to an even greater reduction of the 'hot' transmission of the channels. When the J_3 thres-hold is exceeded, a small increment in the rate can be gained by defocusing and reducing the energy density of the ablation-driving radiation at the target.

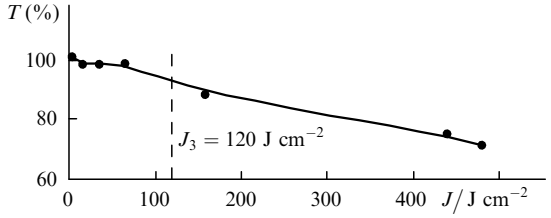

Figure 6. Dependence of the transmission of pure air (without a sample) on the incident energy density for $\tau = 130$ fs.

Similar screening features were observed in the ablation of steel caused by picosecond pulses. Special experiments were performed to reveal the common mechanisms and conditions of the plasma production of this type. The main results of these experiments are presented in Fig. 7. In the experiments, a through opening with a relatively large diameter ($d \gg d_w$) was preformed in a 500-μm thick sample, and then the output energy E_{out} was measured as a function of the incident radiation energy E_{in}. This provided $T_c = 100$ % (the dashed line) and allowed all deviations from this value to be attributed to screening.

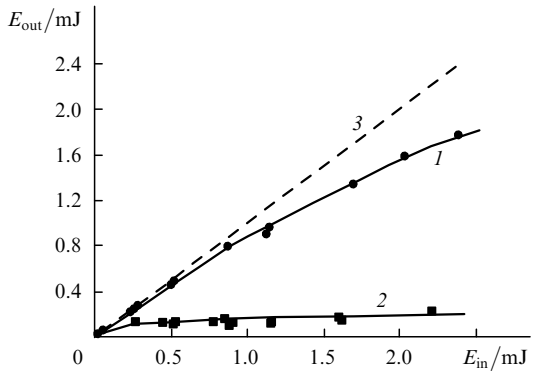

Figure 7. Dependences of the output energy on the incident radiation energy for a through opening in a 500-μm thick sample in the case of a single pulse (*1*) and for $f = 5$ Hz (*3*); curve *3* corresponds to the condition $T = 100$ %.

The greatest screening was observed for a maximum laser pulse repetition rate of 5 Hz. Upon a single-pulse irradiation, with the interval between pulses exceeding the time required for lowering the particle density due to precipitation on the walls or removal from the channel with convective air flows, the transmission level approached 100 %. This time ranged from several seconds to several minutes, depending on the energy and number of the preceding pulses. The energy density $J = 15 - 20$ J cm^{-2}, which corresponds to the intersection of curve 3 and the curve of maximum screening *2*, can be regarded as the screening initiation threshold upon the laser-induced breakdown at the microparticles in the channel for the given repetition rate of picosecond pulses. It follows from Fig. 7 that the plasma screening upon the ablation of steel by picosecond pulses can be as high as 90 %, which is far greater than in the case of femtosecond pulses (see Fig. 4).

The assumption that the screening of intense laser radiation in deep channels is related to the air contamination by ablation microparticles is confirmed by the results of experiments in vacuum. In particular, upon the ablation of steel samples in vacuum at a pressure of 1 Torr, the screening vanished completely and the 'hot' transmission of through channels became equal to the 'cold' one. In addition, the absence of screening inevitably affected the ablation rates. Since 'small' craters can be ventilated efficiently enough by convective flows in the air surrounding the sample, the influence of evacuation increased with crater depths. As a consequence, the ablation rate was pressure-independent in the channels with depths of less than 100 μm. In the channels longer than 500 μm, the ablation rate was higher by one and a half orders of magnitude. This is illustrated by the pressure dependence of the rate of ablation by picosecond pulses presented in Fig. 8.

Of considerable interest is the question of localisation of the plasma cloud which originates in the channel upon the

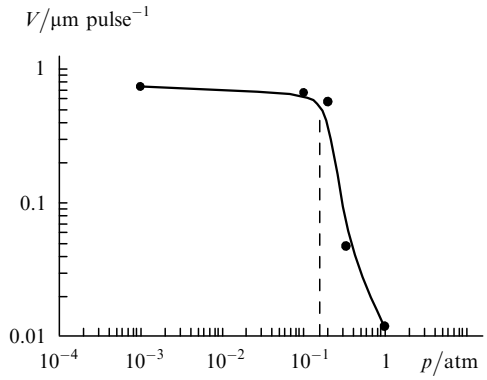

Figure 8. Pressure dependence of the average linear ablation rate for a 500-μm thick sample for $\tau = 300$ ps.

breakdown at the particles. The answer to this question can be obtained by considering the longitudinal channel microsections (Fig. 9). Because the necessary conditions for the gas breakdown inside the channel are a relatively large channel depth and a high enough energy density of the incident radiation, we presented in Fig. 9 the longitudinal sections of the channels of different length whose formation was terminated when the output opening just appeare.

The pictures presented were obtained for an energy density significantly exceeding the threshold of screening ($J =$ 75 J cm^{-2}). In this case, the channel in Fig. 9a is not deep enough for the accumulation of particles, the breakdown does not occur, and the channel diameter is comparable with the diameter of the beam waist. The step-wise channel shape (Fig. 9b) is indicative of two localisation regions of the laser plasma: at the end of the narrow portion of the channel, into which only $\sim 10\,\%$ of the incident energy finds its way, and at the end of the swollen portion in passing to the channel shrinkage, where the remaining $\sim 90\,\%$ of the energy are stored and dissipated in the breakdown plasma. One can see that the regions are spaced at more than 100 μm. In this case, the major part of the incident energy does not reach the bottom and is spent to increase the channel diameter through the interaction with the side walls. When the channels were produced at energy densities not exceeding the screening threshold $J_2 = 15 - 20$ J cm^{-2}, the gas breakdown

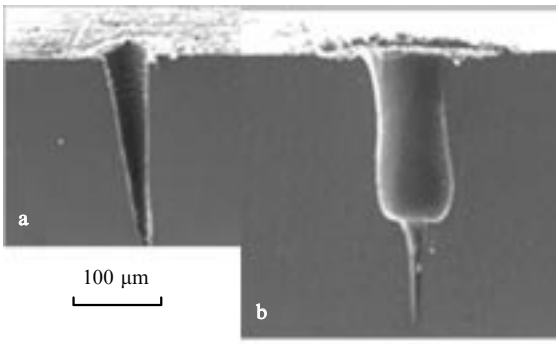

Figure 9. Microsections of channels of different length made in steel by picosecond pulses: a 'shallow' channel (the breakdown at the particles is absent) (a) and a 'deep' channel (there occurs a breakdown at the particles) (b); $J = 75$ J cm$^{-2} \gg J_2$, $\tau = 300$ ps.

did not occur in the region away from the crater bot-tom and a channel of step-wise shape was not formed.

Similar effects are observed in the case of femtosecond pulses, where the plasma–wall interaction is also responsible for the production of broad channels whose diameters are many times larger than d_w. Fig. 10 shows the dependence of the input hole diameter of a 550-μm long channel on the laser pulse energy for $\tau = 130$ fs. The dashed line in the plot denotes the calculated diameter of the Gaussian beam within which the energy density exceeds the threshold level $J_1 =$ 0.05 J cm^{-2}. Because the plasma expansion during the laser irradiation is negligible, a large difference between the measured diameters and the dimensions of the threshold region can be explained by the scattering of a fraction of the incident energy towards the walls by the breakdown plasma, by the short-wavelength radiation from the plasma region [9], and also by its radial expansion after the termination of the laser pulse.

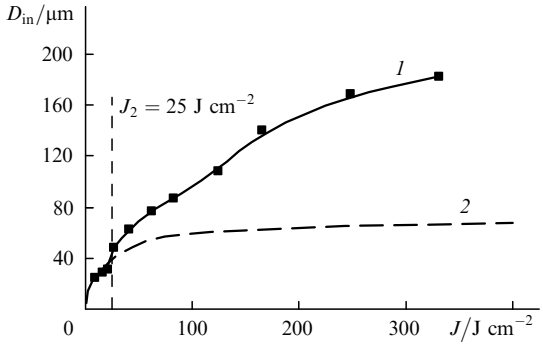

Figure 10. Dependences of the input hole diameter of a 550-μm long channel (*1*) and the diameter of the Gaussian beam (*2*), which corresponds to the threshold J_1 value, on the energy density for $\tau = 130$ fs.

The observed increase in the channel diameter should draw off a significant part of the incident energy and affect the linear ablation rate, resulting in its stabilisation when the threshold value J_2 is exceeded (see Fig. 3). As an illustration of this dependence, Fig. 11 shows the measured rates of femtosecond ablation and some parameter defined as the ratio of the incident energy to the square of the input diameter of the channel being produced (E_{in}/D_{in}^2). Assuming the through openings to be cylindrical enough and the ablation volume proportional to the incident energy, this parameter can be treated as an analogue of the linear ablation rate derived from geometric considerations. One can see that both the calculated and experimental curves have a horizontal portion in the $25 - 120$ J cm^{-2} range. Therefore, it seems that the increment in incident energy in this range for $J_2 < J < J_3$ is spent only for the channel broadening, and does not facilitate the increase in the linear ablation rate.

4. Conclusions

The effect of plasma screening related to the laser-induced air breakdown inside sufficiently deep channels was discovered and studied when the incident energy density considerably exceeded the threshold of surface ablation. The breakdown is initiated by the ablation microparticles residing inside the channels. This type of screening is manifested upon irradiation both by picosecond and femtosecond pulses. In the latter case, the screening is weaker.

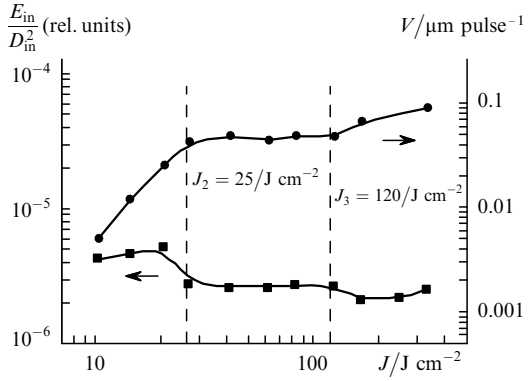

Figure 11. Dependence of the average linear ablation rate and the parameter E_{in}/D_{in}^2 on the energy density of 130-fs laser pulses.

Therefore, plasma in channels can be localised simultaneously in three regions: at the bottom (a surface plasma, the 1st type of screening), at the channel axis some distance away from the bottom (the microparticle breakdown plasma, the 2nd type of screening), and above the surface of a sample (the air breakdown plasma, the 3rd type of screening). The 2nd- and 3rd-type screening initiation thresholds measured for femtosecond pulses are 25 and 120 J cm^{-2}, respectively. The screening upon breakdown at particles (the 2nd type) manifests itself only on reaching a channel aspect ratio of over ~ 1, which may be explained by the removal of the particles from the crater by convective air flows. Due to accumulation of the ablation particles in the channel upon repetitively pulsed irradiation, the magnitude of screening depends on the repetition rate and energy of the preceding laser pulses. The same factors determine the time interval it takes the air in the beam waist to restore the radiation resistance due to removal of the particles from the channel or their precipitation on the walls. The minimal restore time measured in experiment was no shorter than several seconds, thereby making the 2nd type screening unavoidable in the cases of practical significance involving repetitively pulsed ablation of deep channels in air.

Because of a large distance from the bottom, the energy stored and scattered by the breakdown plasma (the 2nd type of screening) does not make a contribution to the increase in the channel depth and is completely transferred to the side walls. This results in stabilisation of the linear ablation rate over a wide range of irradiation energy density. As a result, the channel diameter significantly increases under the action of the expanding and radiating plasma cloud and due to irradiation of the side walls by emission scattered by plasma.

Acknowledgements. This work was supported by the PRIMUS Programme and the Russian Foundation for Basic Research (Grant No. 00-02-17535).

References

1. Preuss S, Demchuk A, Stuke M *Appl. Phys. A* **61** 33 (1995)
2. Stuart B C, Feit M D, Herman S, Rubenchik A M, Shore B W, Perry M D *J. Opt. Soc. Am.* **13** 459 (1996)
3. Momma C, Chichkov B N, Nolte S, von Alvensleben F, Tunnermann A, Welling H, Wellegehausen B *Opt. Commun.* **129** 134 (1996)
4. Von der Linde D, Sokolowski-Tinten K, Bialkowaki J. *Appl. Surf. Sci.* **109–110** 1 (1997)
5. Liu X, Du D, Mourou G *IEEE J. Quantum Electron.* **33** 1706 (1997)
6. Salle B, Gobert O, Meynadier P, Perdrix M, Petite G, Semerok A *Appl. Phys. A* **69** S381 (1999)
7. Kononenko T V, Konov V I, Garnov S V, Danielius R, Piskarskas A, Tamoshauskas G, Dausinger F *Kvantovaya Elektron. (Moscow)* **28** 167 (1999) [*Quantum Electron.* **29** 724 (1999)]
8. Klimentov S M, Kononenko T V, Garnov S V, Konov V I, Pivovarov P A, Dausinger F *Izv. Ross. Akad. Nauk Ser. Fiz.* (4) 145 (2001)
9. Garnov S V, Klimentov S M, Konov V I, Kononenko T V, Dausinger F *Kvantovaya Elektron.* **25** 45 (1998) [*Quantum Electron.* **28** 42 (1998)]
10. Klimentov S M, Garnov S V, Kononenko T V, Konov V I, Pivovarov P A, Dausinger F *Appl. Phys. A* **69** S633 (1999)
11. Prokhorov A M, Konov V I, Ursu I, Mikheilesku I N *Vzaimodeistvie Lazernogo Izlucheniya s Metallami* (Interaction of Laser Radiation with Metals) (Moscow: Nauka, 1988)